SILICON PHOTOMULTIPLIER: A NOVEL TYPE OF PHOTO-DETECTOR WITH SINGLE PHOTON DETECTION CAPABILITY

Giorgio Umberto Pignatel

Dept. of Electronic and Information Engineering DIEI, Perugia, Italy

Key words: silicon photomultiplier, single photon, avalanche breakdown, Geiger mode, photodetector

Abstract: Silicon Photo-Multiplier (SiPM) is a novel type of avalanche photon detector which operates in Geiger mode. It allows great advancement in photon detection and is a good candidate for replacing traditional photomultiplier tubes (PMTs). In this paper the current status of development of a research project founded by the Italian National Institute for Nuclear Physics (INFN) will be presented, in the framework of the DASIPM collaboration which involves several Universities and the Center for Scientific and Technological Research (FBKirst, Trento, Italy). Recent advancements in SIPM technology will be presented, along with some preliminary results and a discussion about possible exploitations in medical and astroparticle physics applications.

Silicijeva fotopomnoževalka: nov tip fotodetektorja s sposobnostjo detekcije posameznega fotona

Kjučne besede: silicijeva fotopomnoževalka, posamezni foton, plazoviti preboj, Geigerjev način, fotodetektor

Izvleček: Silicijeva fotopomnoževalka (SiPM) je nov tip plazovitega prebojnega fotodetektorja, ki deluje v Geigerjevem načinu. Nova fotopomnoževalka predstavlja velik napredek pri detekciji fotona in je dober kandidat za nadomestitev tradicionalne fotomultiplikacijske cevi (PMT). V prispevku bo predstavljen trenutni položaj na projektu, ki je podprt od Italijanskega nacionalnega instituta za nuklearno fiziko (INFN) v okviru sodelovanja DASIPM, ki vključuje nekatere univerze ter Center za znanstvene in tehnološke raziskave (FBKirst, Trento, Italy). Predstavljeni bodo novi dosežki na področju SIPM tehnologije, skupaj z nekaterimi preliminarnimi rezultati ter obravnavo možnih aplikacij v medicini in astrofiziki.

1 Introduction

Efficient detectors for low-light level (LLL) and photon counting applications are today required in a large variety of fields including astroparticle physics, nuclear medicine and high-energy physics. For such experiments, photon detectors typically employed are vacuum photon detectors, i.e., photomultiplier tubes–PMT, micro-channel plate photo-multipliers –MCP, hybrid photodetectors–HPD /1-3/. The main advantages of such devices are high internal gain (10^6-10^7), very good timing resolution (tens or hundreds of ps) and good single photoelectron resolution. However, these devices have low quantum efficiency limited by the photocathode materials, high operation voltages, they are sensitive to magnetic fields and the vacuum technology used for their fabrication confers them a bulky shape and sensitivity to handling.

The search for new photon detectors which can over-come the drawbacks of vacuum photon detectors has lead to the development of solid state photon detectors (PN or PIN photodiodes, avalanche photodiodes–APD and avalanche photodiodes operating in linear Geiger-mode–GAPD or SPAD) /4, 5/. These solid-state devices have important advantages over the vacuum ones, namely higher quantum efficiency, lower operation voltages, insensitivity to the magnetic fields and robustness and compactness. The step-by-step evolution of solid-state photon detectors was mainly determined by their internal gain: a PIN has no gain, an APD has a gain of few hundreds and the GAPD gain is 10^5-10^6. A gain comparable with that of the vacuum photon detectors allowed the GAPD to achieve single-photon sensitivity and to be used in LLL applications (~10^7 photons/mm^2/sec).

Essentially, a GAPD is a p-n junction that operates above the breakdown voltage. At this bias, the electric field is so high that a single charge carrier injected into the depletion layer can trigger a selfsustaining avalanche (so-called Geiger breakdown). The Geiger breakdown mechanism in avalanche diodes was studied several years ago /6, 7/ and important progresses on suitable quenching circuits al. /8/. However, a GAPD has the disadvantage that it acts as a binary device, having a standardized output signal independent of the number of incident photons. A new structure called Silicon Photo- /9-10/ overcome this inherent limitation bringing together on the same substrate many micro-cells connected in parallel, in which each micro-cell is a GAPD in series with its integrated quenching resistor. Therefore, the SiPM acts as an analog device with an output signal representing the sum of the signals from all fired micro-cells and it becomes a suitable solid-state device for LLL detection and photon counting applications, including the detection of the space radiation in astroparticle physics, medical imaging in nuclear medicine, and calorimetry in high-energy physics /11, 12/.

At the beginning of 2005, within collaboration between the Italian National Institute for Nuclear Physics (INFN) and the Center for Scientific and Technological Research of Trento, Italy (FBK-irst), a 3-year project aimed at the development of silicon photomultipliers was launched. Within

this project, the role of FBK-irst was the technological development and the electrical characterization of silicon photomultipliers, whereas the role of INFN was mainly focused on the application of such devices, with special emphasis on Calorimetry, time-of-flight (TOF) measurements, and PositronEmission Tomography (PET).

In this paper the FBK-irst activity in developingand producing SiPMs will be reviewed, and theongoing activity of the DASIPM collaboration /13/:"Development and Applications of Silicon Photo-Multipliers" - which involves the Universities ofPisa, Perugia, Trento, Bologna and Bari - will bereported.

2 Detector description

Fig.1 shows the picture of a SiPM device. It is composed by a matrix of 25x25 photo-diode cells with an area of 40x40 μm^2 covering a surface of 1x1mm^2. The device is realized on a low-resistivityp+-type substrate (500μm thick).

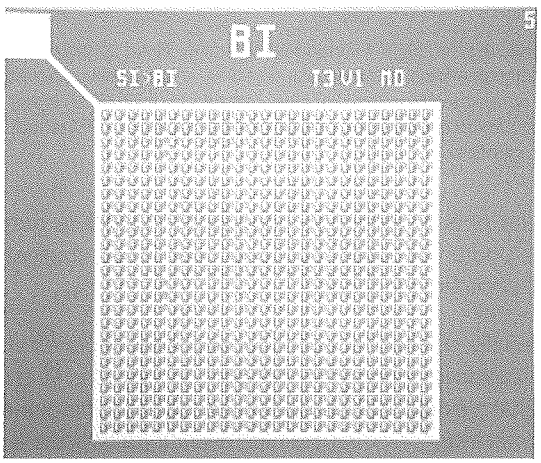

Fig. 1: Photograph of the first prototype of SiPMfrom FBK-irst.

The structure of each diode consists of an asymmetric shallow junction (n+p) implanted in a thin (~4μm) lowly doped p-type epitaxial layer. The junction is created by an Arsenic implantation and is located at about 100nm from the top silicon surface.The breakdown voltage value is fixed by a further Boron implantation. The doping profiles and the dielectric layers deposited on the silicon surface are designed to enhance the photon-detection efficiency in the short wavelength region (420-450nm) /14/. It must be emphasized that each micro-pixel has about 6Pm wide dead area along the edges which is needed to accommodate the structures for the reduction of the lateral fields (guard rings) and for the electrooptical isolation (V-groove, fig.2).

A simple equivalent circuit of the SiPM is shownin fig.3. A reverse bias voltage (Vbias) is applied to all junctions through the common substrate electrode to deplete the epi-layer and the induced current is read on the resistor side electrode.

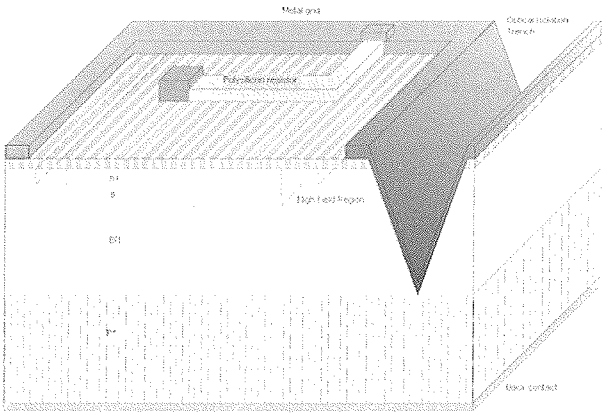

Fig. 2: Schematic of a single GAPD cell.

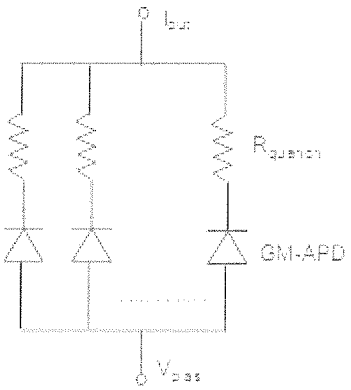

Fig. 3: Simplified equivalent circuit of a SiPM.

2.1 Principle of operation

When the diodes are biased (VB) at few volts above breakdown (VBD) the electric field in the junction region is so high that any carrier, generated either thermally or by photons and drifted in that region, may trigger a self-sustaining avalanche breakdown. While a swift current pulse grows to a macroscopic level in a very short time (~500ps) it flows through a series resistor RQ which limits the current to about 10μA and develops a voltage drop which quenches the avalanche by reducing the bias voltage. Thereafter the original over-voltage ($\Delta V=V_B-V_{DB}$) isexponentially recovered within a time constant $R_Q x C_D$. At room temperature the rate of thermally generated carriers is of the order of 0.1-1.0MHz/mm2 (dark-count rate) and that represents the limitin gfactor (noise level) of the device.

3 Detector characterization

This section reports the characterization of the single micro-pixel. It is divided in two parts describing the static and the dynamic functional characteristics, respectively.

3.1 Static Characterization

Several information concerning the behavior of the SiPM can be inferred from static I-V measurements

3.1.1 Forward characteristic

The forward I-V characteristic of a single micro-cellor a whole SiPM allows us to extract the value of the quenching resistor RQ.

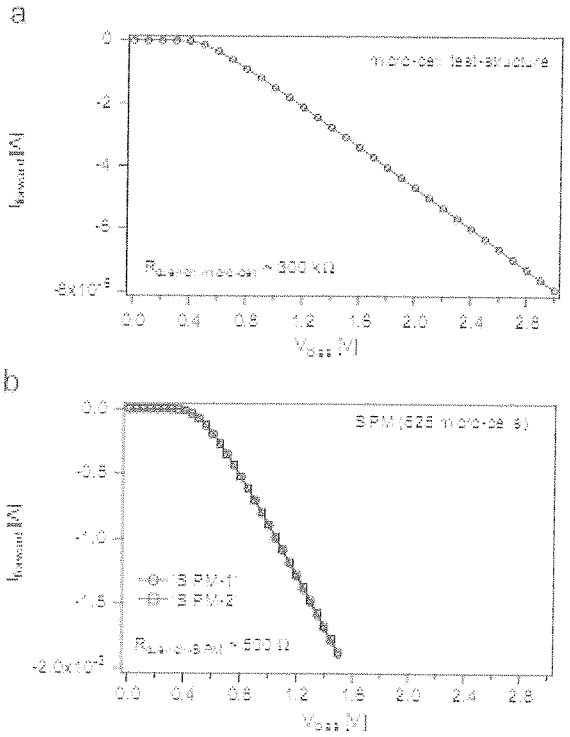

Fig. 4. I-V forward characteristics of (a) a single micro-cell test structure and (b) two SiP

For example, for the device reported in fig.1, the value of the quenching resistor extracted from the forward characteristics of the micro-cell test structure is of 300kΩ, whereas for the SiPM a value of ~500Ω has been determined (see Figs. 4a and 4b), in good agreement with the expected value (RSiPM =Rmicro-cell / Nmicro-cell, with Nmicro-cell=625)/14/.

Measurements have been repeated on a statistically meaningful number of devices on each wafer, showing a very good uniformity of the resistance values and confirming the reliability of the polysilicon technology used for the Rquench fabrication.

3.1.2 Reverse characteristic

The reverse characteristic contains precious information on the functionality of the SiPM. First of all, the breakdown voltage can be extracted. Forexample, in fig.5 /15/ it is clearly visible that V_{BD} is about 31V, with a uniformity which has been estimated to be within ±0.5V from SiPM to SiPM, inspite of the fact that the reverse current above V_{BD} can differ by a factor of about 10 from pixel-to-pixel, as reported in fig.6.

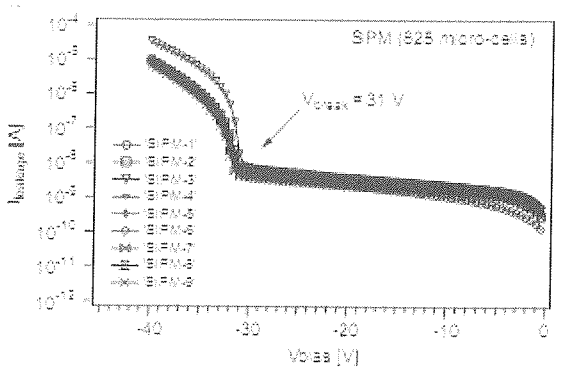

Fig. 5. Reverse I-V characteristics of 9 SiPM taken from the same wafer.

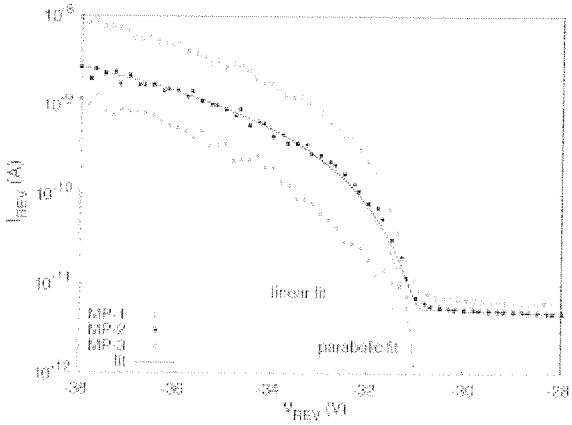

Fig. 6. Close view of the I-V reverse characteristic of a SiPM around breakdown. The reverse current of two micro-pixels multiplied by 625 is shown as well.

Concerning the current level below the breakdown, that is determined by the carriers generated both in the bulk as well as on the surface of the depleted region around the junction. Fortunately, the latter do not contribute to the dark-count rate, as it is orders of magnitude lower than that predicted by the measured current level.

Concerning the current behavior above breakdown, it is interesting to note that it follows a parabolic law up to voltages of several Volts above breakdown. This behavior can be explained considering that the DC current flowing through the GAPD in this region (above breakdown) is given by the average charge generated from spontaneous (thermally generated) breakdown in 1s. In an ideal device, this value is given by the charge contained in one pulse (Q) timesthe number of pulses per second (dark count rate).

$$I_{DC} = Q \times DCR$$

The first term represents the gain $G = Q/e$ of the GAPD since it is the number of carriers generated by a single carrier triggering the avalanche. The I-V curve is parabolic because, as it will be shown in thefollowing sections, both the gain and the dark countrate grow linearly with the bias voltage.

3.2 Dynamic Characterization

The signal coming from the micro-pixel is expected to show a very fast leading edge, determined both by the avalanche spreading and by the discharge of the diode capacitance C_D through the series resistance R_S (which includes the resistance of the neutral region of the semiconductor and the space-charge of the avalanche junction), and a slow exponential decay, determined by the time constant

$$\tau = R_Q \times C_D$$

C_D can be estimated from the geometry of the microcell applying the parallel-plate capacitance equation. Considering a 4μm thick epitaxial layer and a device area of 40x40μm, an indicative value is 50fF/pixel gives a recovery time constant of 17ns. A slightly longer recovery time can be expected, taking into account the parasitic capacitance CQ of the polysilicon quenching resistor which lies on top of the photo-diode area.

3.2.1 Dark pulse measurements

Several information on the dynamic characteristic of a SiPM can be inferred from simple dark pulse measurements.

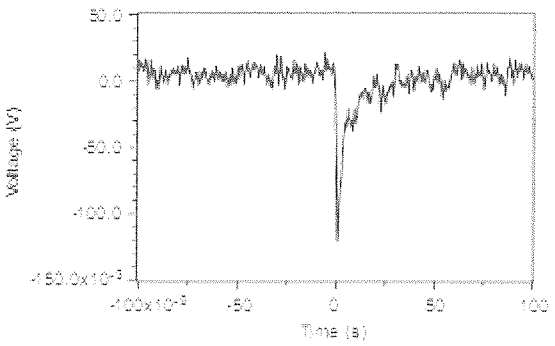

Fig. 7. Dark pulse from a SiPM micro-cell biased at 4V above V_{break}.

Fig.7 shows a typical dark pulse measured with a wide-band digital oscilloscope. A rise time of less than 1ns and a recovery time constant of a 20ns demonstrate the fast timing characteristics of the SiPM signal. The total recovery time, defined as the time needed to recharge the diode to 99% of the bias voltage, is about 80ns, and this parameter determines the maximum allowed photon counting rate.

3.2.2 SiPM's Gain

The Geiger signal from one pixel is determined by the charge ($Q_{PIXEL} = C_{PIXEL} \times \Delta V$) accumulated in the pixel capacitance CD biased at an overvoltage:

$$\Delta V = V_{BIAS} - V_{BD}$$

The overvoltage is of the order of few Volts and C_{pixel} is typically 50fF; so Q_{pixel} is of the order of 150fC or 10^6 electrons. One pixel signal on 50Ω load resistor corresponds to a pulse amplitude of ~ 1mV which can be detected by a wide-band oscilloscopeeven without a preamplifier near the detector. A direct measurement of Q_{pixel} can be obtained integrating the pulse signal.

Fig.8 shows the *spectra* obtained integrating the pulses reported in Fig.7 for an integration time of 100ns (which includes the whole signal) at different bias voltages.

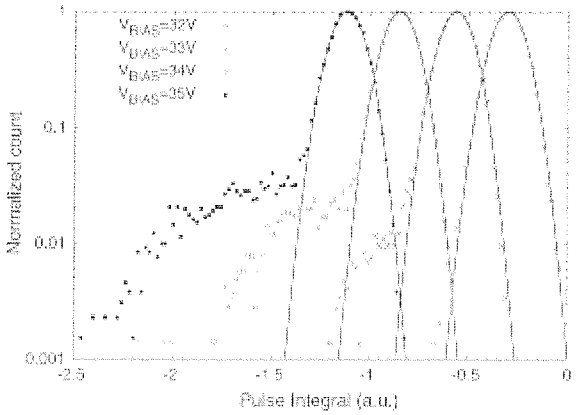

Fig. 8. Spectra of the signal charge (integration time 100ns) at four bias voltages.

Each distribution has a dominant peak that can be very well fitted by a Gaussian distribution. The centroid of the Gaussian is the most probable charge generated in one pulse and grows linearly with the bias voltage, in contrast to the exponential voltage dependence of the gain of APDs. The variance of the Gaussian is determined by two contributions: the noise introduced by the read-out system and the fluctuations of the GAPD gain. The tail in thedistribution of Fig.8 is due to multiple events which occur in the 100ns integration time.

The linear dependence of the gain with bias voltage is clearly visible in Fig.9 showing the charge expressed in number of carriers as a function of the bias voltage along with a linear fit.

The intercept with the x-axis corresponds very well to the breakdown voltage value that was previously extracted from the I-V characteristics. The slope is proportional to the capacitance of the micro-cell, which, as expected, is about 50 fF.

3.2.3 After pulsing

The pulse reported in Fig.7 represents the ideal case in which a single event is detected in the observation time slot. In practice, while acquiring a SiPM signal, there is a certain probability that a secondary pulse is emitted after a short time. This phenomenon is called "after-pulsing" and is attributed to the release of carriers which have beentrapped in the band-gap of the semiconductor during the main avalanche, and which are re-emitted after a characteristic decay time, and then can trigger a second breakdown /16/

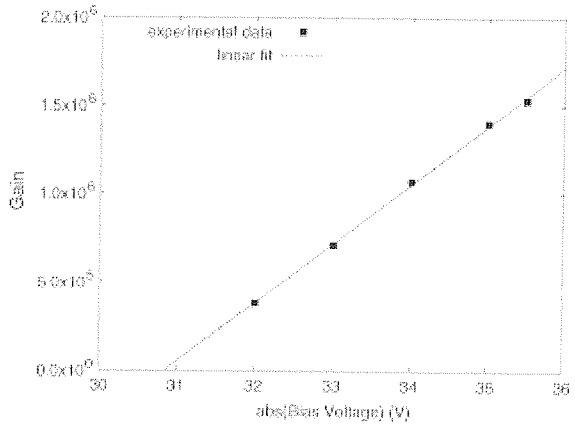

Fig. 9. Gain of the GAPD as a function of the bias voltage.

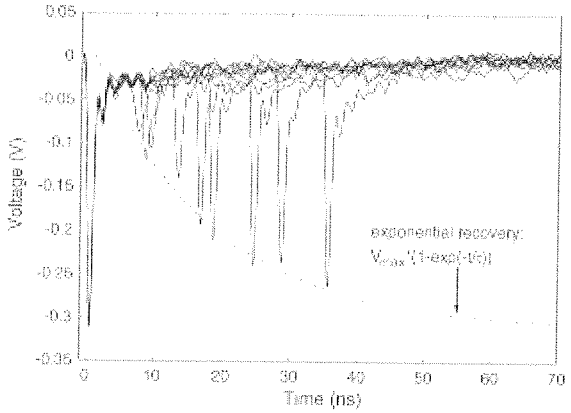

Fig. 10. Collection of pulses presenting an after-pulse event (V_{bias} = 35V).

A collection of such events is reported in fig.10/15/. The main pulses are exactly overlaid at time 0, whereas the secondary pulses are randomly distributed after the primary. The height of the second pulse depends on the relative position (intime) with respect to the first one, because the diode voltage is still slowly increasing towards V_{BIAS} andconsequently the gain changes according to the plot in Fig.9. It is interesting to note that, from the convolution of the secondary pulse peak (dashed line), a recovery time constant consistent with the previously reported $R_Q C_D$ can be extracted.

3.2.4 Cross-talk

Another contribution to the "noise" of a SiPM is cross-talk. Since a SiPM is composed of hundreds (or even thousands) of pixels, there is a certain probability that an avalanche breakdown generated in one pixel can trigger the avalanche in another, adjacent pixel. It has been shown /17/ that this phenomenon is due to infrared optical photons which are emitted during the main avalanche and reach the adjacent pixels not only in the horizontal plain, but also by reflection from the back side of the device. The emission probability of optical photons from hot carriers in an avalanche breakdown was estimated tobe $3x10^{-5}$ /16/; therefore, it can be argued that a 30 optical photons are emitted per pulse with a gain of 10^6. An optical cross-talk coefficient $K_{2/1}$ can be defined as the probability for a second pixel to be-fired. It has been shown that this coefficient is linearly dependent on the gain and can vary from a few per cent up to 35% /18/. Since the velocity of optical photons in Silicon is ~ 100μm/ps, the optical cross-talk is seen at the output of a SiPM as a single pulse with amplitude 2x, 3x, ...etc.

Fig.11 is an example of the output signal from a SiPM which exhibits single pulses, after-pulses, and cross-talk.

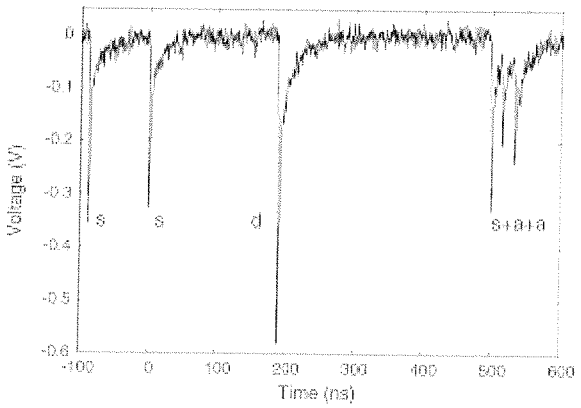

Fig.11. Output signal from a SiPM presenting single pulses (s), double pulses (d), and after-pulses (a).

The cross-talk effect is visible as a tail in the spectra of a signal charge, as reported in Fig.8. From inspection of fig.8 it can be argued that, for FBK-irst SiPMs, the cross-talk is less than 5%.

3.2.5 Dark Count Rate

The dark count rate can be measured either with a digital oscilloscope with counting capability, or with a counter inserted after a pulse-height discriminator. Due to the short rise time of the pulses and to their good stability, it is not necessary to use a constant fraction discriminator.

Fig.12 shows the measurement of a SiPM dark count rate as a function of pulse amplitude (threshold level) at room temperature.

The dark count rate for a threshold of 1 photoelectron (p.e.) level varies between 1 and 3MHz for ΔV values from 1.5 to 3.5V. At 3 p.e. level the dark count is just few kHz at ΔV=1.5V and ~1 kHz at 3.5 V.

That means that DCR is a limiting factor for single photon detection, but not for low-light level illumination, when the number of hitting photons is > 3 or 4.

4 SiPM parameters

The performance of a Silicon Photomultiplier is affected by two important parameters: photon detection efficiency (PDE) and Linearity (dynamic range).

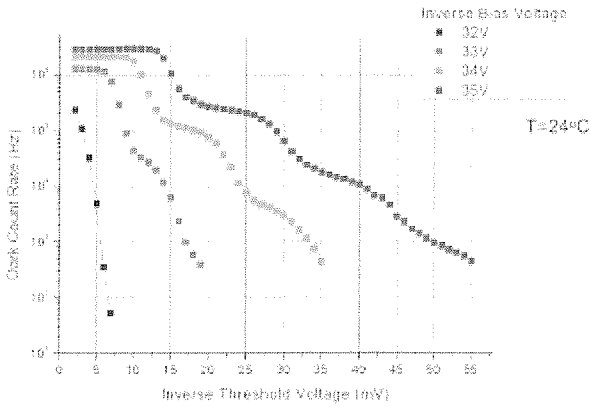

Fig.12. SiPM dark count rate as a function of puls eamplitude (threshold) for different bias voltages.

4.1 Photon detection efficiency – PDE

PDE can be defined as the probability that an incident photon generates a useful output signal. The detection efficiency of a SiPM is given by the product of 3 terms: the quantum efficiency (QE), the probability to initiate an avalanche breakdown (Pa),and the geometrical - or fill - factor (GF).

$$PDE = QE(\lambda) \times Pa(V) \times GF$$

4.1.1 Quantum efficiency – QE(λ)

The quantum efficiency represents the probability for a photon to generate an e-h pair. It is given by the product of 2 factors: the transmittance of the dielectric layer on top of the silicon surface and the intrinsic silicon QE. Both are wavelength dependent. The former can be maximized by implementing an anti-reflective coating (ARC). The second represents the probability for a photon that has crossed the dielectric layer to generate an e-h pair in the active area of the device. In a conventional n+/p/p+ diode, the active layer is roughly limited on top by the undepleted n+ doped layer, whereas on the bottom it is limited by the p+ layer used for the ohmic contactor by the highly doped substrate in case of epitaxial substrates. Indeed, when a pair is generated in those regions, there is a high probability for electrons andholes to recombine by means of Auger or Shockley-Read-Hall (SRH) processes. For short wavelengths, the problem is focused in the top layer. As an example, a 420nm light is almost totally absorbed in the first 500nm of silicon, which, for non-optimized fabrication processes, is usually well inside the undepleted layer.

4.1.2 Avalanche probability – Pa(V)

There is a finite probability that a carrier swept or generated within the space-charge region triggers an avalanche breakdown. In case of a photon generated event, 2 carriers are created travelling in opposite directions. Both contribute to the triggering probability as:

$$Pa = Pe + Ph - PePh$$

where Pe and Ph are the electron and hole avalanche initiation probabilities respectively /19, 20/. These terms depend on the impact ionization coefficients of electrons (α) and holes (β) which are strongly dependent upon the electric field (applied bias voltage). The ionization coefficient for electrons is higher than that for holes (e.g., at $5x10^5$V/cm, α is about twice than β)

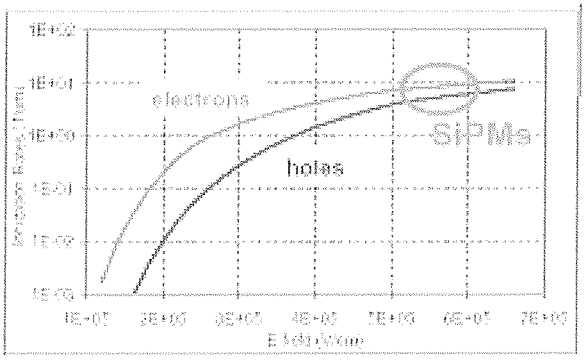

Fig.13. Ionization rates of electrons and holes in silicon /Grant SSE 16, 1973/.

4.1.3 Geometric factor – GF

The ratio between the active area and the total area of the device is a critical issue in SiPMs. The reason is that each GAPD cell is surrounded by a dead region determined by the guard ring and the structure preventing optical cross-talk. Considering that the area of a cell can be very small (of the order of 30x30μm^2) even few microns of dead region around the cell have a detrimental effect on the geometrical efficiency. Presently, the fill factor of FBK-irst SiPM is limited to 0.2-0.33 for cell areas ranging from 30x30μm^2 to 50x50μm^2.

As an example, the PDE of a SiPM with fill factor=0.2 is reported in fig.13 /21/.

The PDE dependence on the bias voltage has to be attributed to the avalanche initiation probability. The dependence on the light wavelength is a mixed contribution from Pa and QE. To separate the two contributions the quantum efficiency of some diodes extracted from the same wafers, which have the same anti-reflecting coating and doping profiles have been measured (see fig.15 from ref /21/).

It is worth while noting that in a conventional n+/p/p+ device structure, there is more chance that the avalanche breakdown is initiated by electrons at long wavelength, and by holes at short wavelength, as the photon absorption length in silicon ranges from 0.01μm to few μm for wavelengths 300nm<λ<700 nm.

4.2 Dynamic range & Linearity

In principle, the dynamic range of a SiPM is equal to the number of micro-pixels contained in a macrocell. Howev-

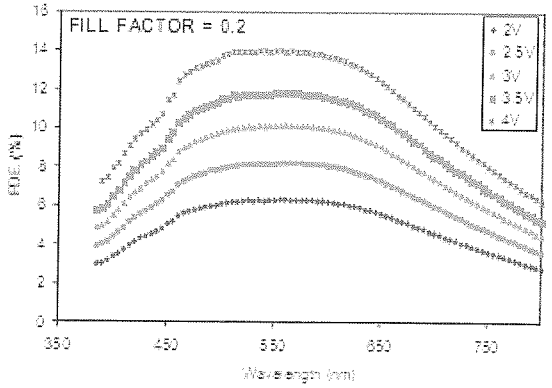

Fig.14. PDE vs wavelength of a SiPM measured at different over-voltages: from 2V to 4V.

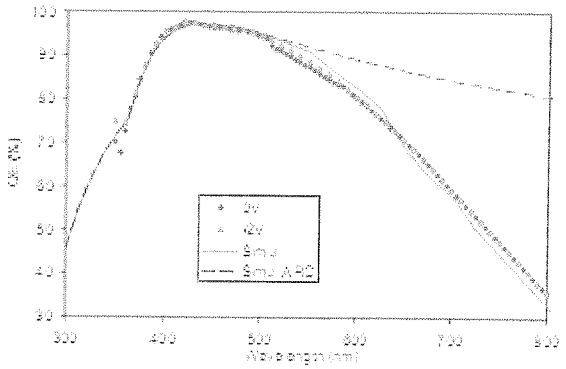

Fig. 15. QE vs wavelength of a 1mm² diode having the same doping profiles and anti-reflecting coating of the SiPM

er, the output signal amplitude is proportional to the number of incident photons only if each micro-cell is hit by a single photon during the recovery time of the micro-cell. When the number of photons increases, there is a certain probability that two or more photons hit the same cell, thus producing the same signal. It can be shown that the dependence of the SiPM signal (N_{SiPM}) on the number of incident photons (N_{ph}) follows a Poisson distribution:

$$N_{SiPM} = N_{cells}\left[1-\exp\left(\frac{N_{ph}\times PDE}{N_{cells}}\right)\right]$$

where N_{cells} is the total number of cells of the SiPM. Fig.15 shows the saturation effect measured on 5FBK-irst SiPMs /22a/.

The linearity of the SiPM response is crucial for energy calibration when the SiPM is coupled to a scintillator which exhibit high light yield (thousands of photons) or long decay time (hundred of ns).

4.3 Temperature dependence

The temperature dependence of the gain of a SiPMis related to the leakage current and the dark count rate of the detector:

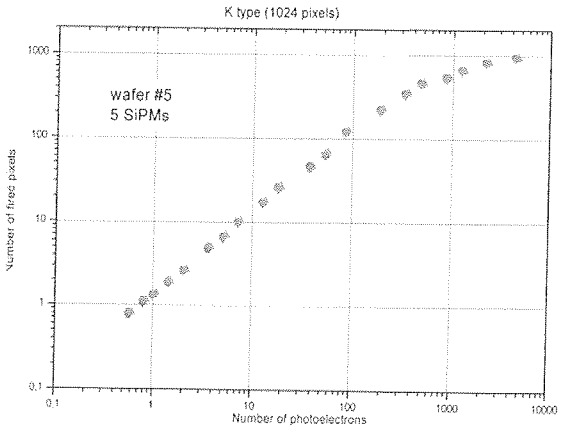

Fig. 16. Non-linear output saturation of 1024 pixel /1.0 mm² FBK-irst SiPMs as a function of incident photon number /22a/

$$G(T) = \frac{I_{leak}(T)}{e\times DCR(T)}$$

where e is the electron charge and I_{leak} is the rms dark current. A picture of such dependence is reported in fig.16 /23/. It has been shown that the gain is linear with the over voltage (V_{OV}) independently of the temperature. However, if the bias voltage is kept constant, an effective variation of the gain is observed, as reported in fig.17, due to the fact that the breakdown voltage changes:

$V_{OV}(T) = V_{BIAS} - V_{BD}(T)$

For a pure avalanche process /5,6/, the temperature dependence of the breakdown voltage can be approximated as:

$$V_{BD}(T) = V_{BDO}[1 + \beta(T - T_O)]$$

where V_{BDO} is the breakdown voltage at room temperature (T_O) and β is a linear coefficient.

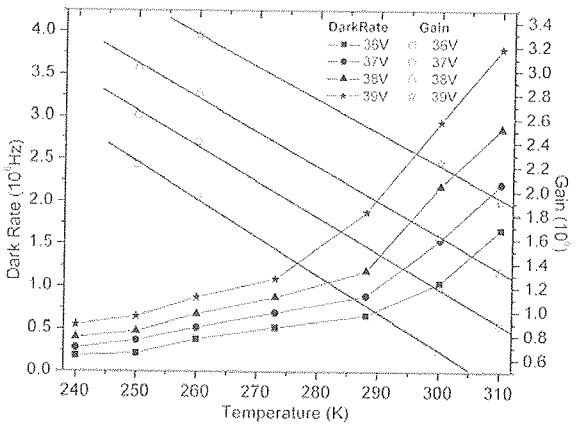

Fig. 17. SiPM gain and dark rate as a function of temperature.

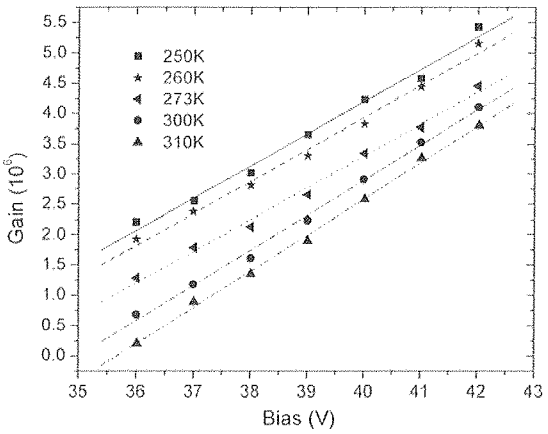

Fig. 18. SiPM gain as a function the bias voltage at different operating temperatures.

For the samples reported in fig.19 this model fit the experimental data for β equal to 2 ± 0.06810^{-3} K^{-1}.

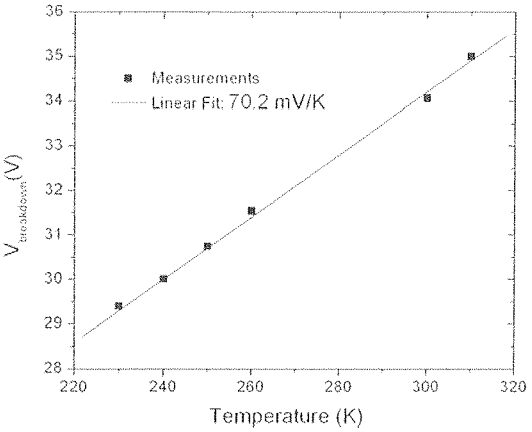

Fig. 19. SiPM breakdown voltage as a function of temperature.

5 Readout electronics

As previously mentioned, the output signal of a SiPM is a short pulse whose amplitude on a 50 Ω load resistor is expected to be of the order of 1mV per fired pixel. Such signal can be displayed on a wide-bandwidth digital oscilloscope, even without amplification, as reported in fig.19.

However, when connected to a threshold discriminator in photon counting or spectroscopy applications, the SiPM signal requires some pre amplification.One possibility is to use a wide-band voltage amplifier; however, as the SiPM behaves like a current pulse generator, a trans-impedance amplifier (TIA) is preferable for keeping the input impedance low and the response time very short.

The use of discrete components for the read-out electronics is convenient for a single photon detector, and eventually for a limited array of photon detectors. However, for applications where a large number of arrays or matrixes of

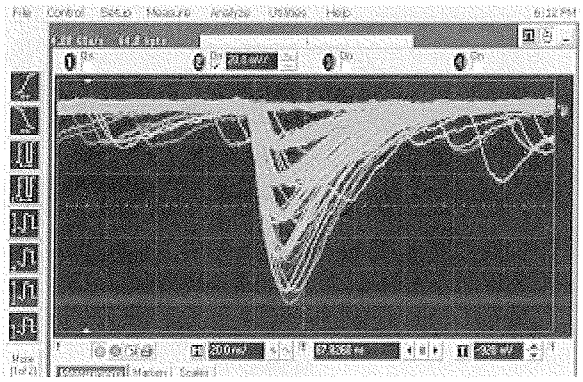

Fig. 20. Example of single photoelectron levels as observed on an oscilloscope (courtesy of SensL)

SiPMs is required,the use of a dedicated reado-ut circuit (ASIC) is mandatory.

In the framework of the DASIPM collaboration, the research unit of Bari is responsible of the design of an innovative read-out chip optimized for the FBK-irst SiPM. Preliminary results have been presented at the Nuclear Science Conferences /24, 25/. First of all, a spice model of the SiPM has been extracted which takes into account internal and external parasitic components /26/. Secondly, a first prototype of a single channel, front-end circuit has been realized in AMS 0.35um CMOS technology which exhibits an input current buffer stage and a current discriminator /27/.

At the present moment there is no read-out chip available on the market specifically designed for SiPM devices. However, it is worth mentioning that in the framework of the international CALICE collaboration for the realization of a Hadrons Calorimeter (HCAL) at the International Linear Collider (ILC, CERN-CH), the electronic group of LAL-Orsay (CNRS-FR) is developing a 36-channel SiPM read-out ASIC called "SPIROC" /28/.

6 Applications

SiPM is a compact, rugged, solid state detector insensitive to magnetic fields /29/. For these reasons it is a good candidate for replacing bulky vacuum photomultiplier tubes (PMTs) in low-light level applications. The number of such applications is enormous in the field of high energy physics (HEP), astroparticle physics, biology, oncology and nuclear medicine. An excellent overview of the potential applications of SiPM in HEP experiments can be found in ref /30/. Biology and oncology applications include protein fluorescence, molecular imaging, and single photon emission computed tomography (SPECT). The DASIPM collaboration is focused on a stroparticle physics and positron emission tomography (PET). Astroparticle physics includes intillating fiber tracking of high energetic particles,time of-flight measurements (TOF), Cerenkov imaging of cosmic rays /22b/. In this section some results concerning gamma-ray spectroscopy from radioac-

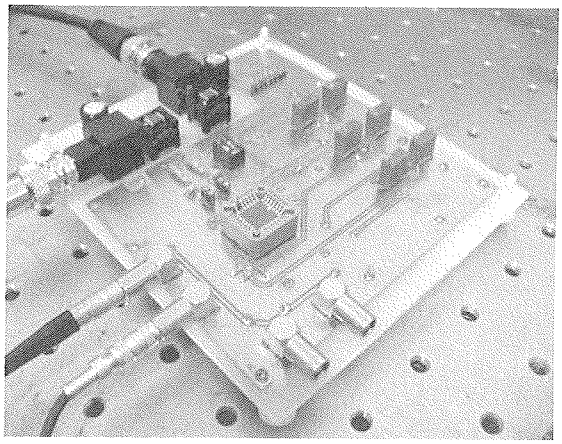

Fig. 21. Evaluation board of the first ASIC prototype

tive sources by means of LSO scintillators coupled to SiPM for PET/MRI and small animal imaging will be reported.

6.1 Energy resolution

At low level of illumination a good resolution is given by the ability of the detector to distinguish between single photo-electrons (s.p.e.).

In fig.21 a s.p.e. spectrum has been obtained illuminating the device with a pulsed LED at very low light intensity. The peaks corresponding to 1 to 9 p.e. can clearly be distinguished, showing the excellent s.p.e. resolution of these devices /31/.

For particle tracking and for PET applications the SiPM is coupled to a scintillator who converts a single high energetic (gamma) photon into a shower of optical photons. The efficiency of the conversion process depends upon the properties of the scintillating materials, i.e., atomic density, light yield, decay time and emission wavelength. Cesiumor Yttrium doped Lutetium Oxyortosilicate (LSO) is a good material for PET, because it has a high density (7.2gr/cm^3), high luminosity (>26000ph/MeV), short decay time (~40ns), and a max emission wavelength of 420nm (blue).

In positron emission tomography the position of the emitting radioactive source is reconstructed from the coincidence of two 0.511MeV gamma photons which are emitted at 180° by positron annihilation.

A spatial resolution of less than 1mm over a distance of several cm can be achieved, provided that the 511KeV spectrum peak can be separated from the low energy tail that is generated by Comptons cattering of gamma photons in living tissue.

Another difficulty is that, while keeping a submillimeter-space resolution, we would like image are latively large area of the body tissue. Finally, the large number of photons emitted by the scintillator can saturate the detector. The solution is a large area detector, or a matrix of many pixilated detectors.

Fig.22 shows a SiPM matrix composed of four (2x2) pixel elements in a common substrate, with a 1mm^2 LYSO scin-

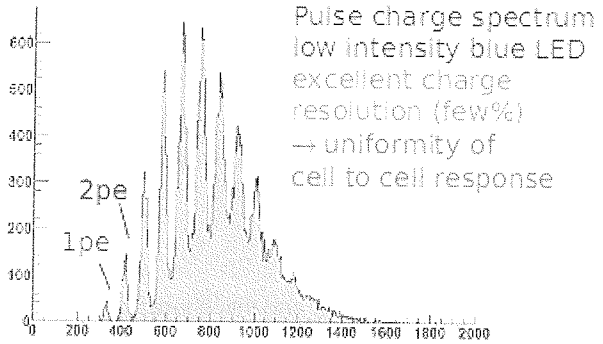

Fig. 22. Single photo electron spectrum. The first peak is the pedestal. The other peaks correspond to 1, 2..p.e.

tillator placed in the middle. Fig.23 shows the ^{22}Na spectrum obtained summing the signal from the four adjacent pixels /32/.

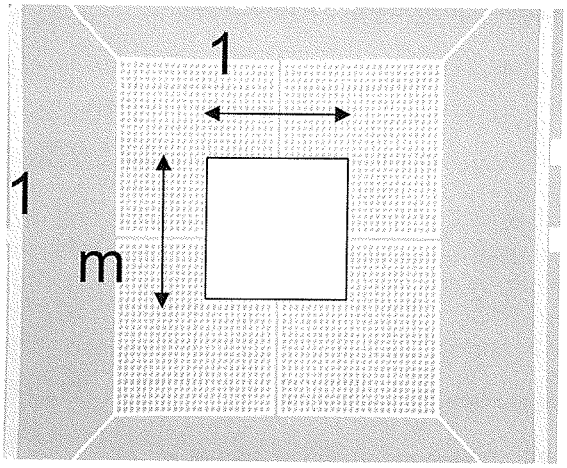

Fig. 23. SiPM matrix of 2x2 pixels with at 1 x 1 x 10mm^3 LSO cubic scintillator placed in the middle

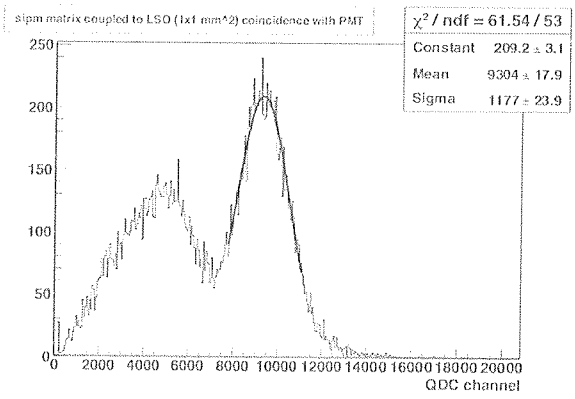

Fig. 24. ^{22}Na energy spectrum obtained as the sum of four adjacent SiPM.

The energy resolution is only 30% FWHM, but the sodium peak is well defined and can easily separated from the Compton tail by setting the threshold of the discriminator above 7000 channels.

A much better resolution of 16% FWHM has been obtained on a 3x3mm^2 SiPM (3200 sub-pixels) coupled to a cubic 3x3x3mm^3 LYSO crystal /33/.

The results obtained so far are very promising, and support the idea that large area detectors can be fabricated to meet the specifications of PET/MRI.

6.2 Timing resolution

The SiPM is a fast detector, and this characteristic can be exploited in TOF or TOF-PET experiments.

6.2.1 Single photon timing resolution

The intrinsic timing resolution of a SiPM has been evaluated at the single photoelectron (p.e.) level, illuminating the device with a pulsed laser with 60 fs pulse width at 80 MHz rate (T=12.34 ns) with less than 100 ps jitter /31/. The time difference between contiguous signals is evaluated and plotted, and there sulting distribution is fitted with a Gaussian function (fig.25, ref /34/).

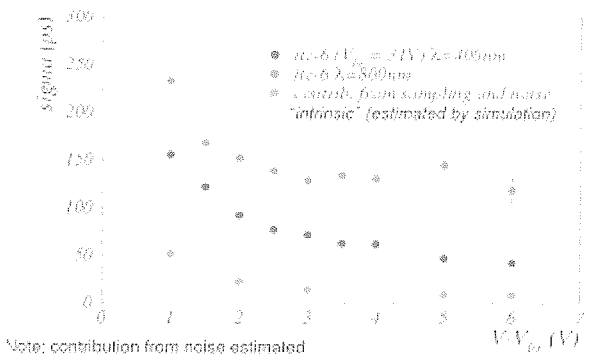

Fig. 25. Timing resolution of a SiPM at single photoelectron level as a function of the overvoltage measured at two different wavelengths

The measurement has been performed with blue light (400±7nm) and red light (800±15nm). An intrinsic timing resolution of ~ 60 ps rms has been measured for blue light at 4V overvoltage. The value for red light is higher, since the photons penetrate deeper in the detector and the carriers drift for a longer time before reaching the avalanche region.

6.2.2 Multi photon timing resolution

When more than 1 p.e. is generated in the SiPM, the timing resolution improves as $1/\sqrt{Npe}$, according to the Poisson statistics. At 15p.e, the timing resolution is ~ 20 ps rms.

6.2.3 Coincidence timing resolution

The time coincidence of events occurring in two different detectors is measured with two discriminators. One select the full energy event and generates the trigger signal; the second generates the coincidence signal that will be em-

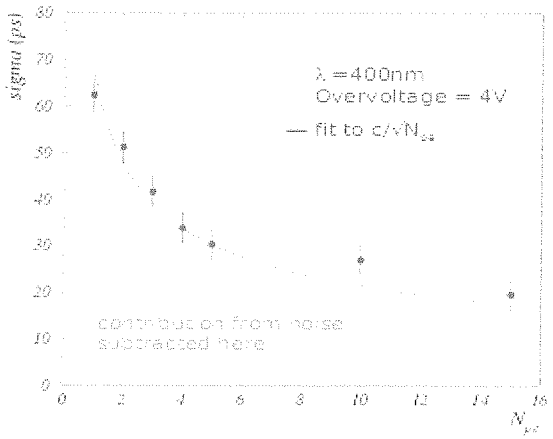

Fig. 26. Timing resolution of a SiPM as a function of photogenerated electrons (Npe)

ployed to estimate the time jitter between the two devices. The time distribution obtained for two LSO crystals coupled to two SiPMs is shown in fig.26.

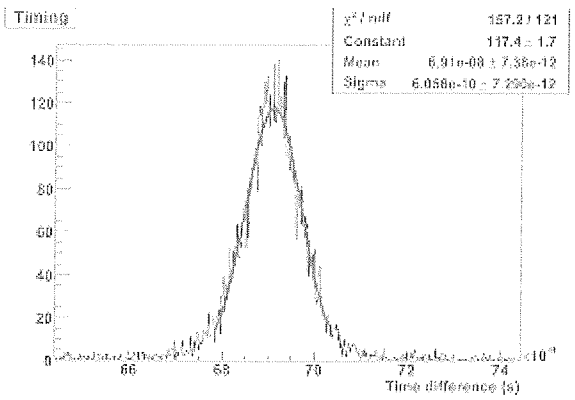

Fig. 27. Coincidence timing resolution of two SiPMs coupled to LSO crystals.

The timing resolution is 600ps sigma (1.4nsFWHM); a value well below the typical 10ns resolving time used in PET.

Finally, fig.26 shows the 511KeV Na spectrum obtained with a 1mm x 1mm x 10mm LSO crystal coupled to a SiPM, operated in coincidence with another device. In these conditions an energy resolution of 21% FWHM was obtained / 33/.

7 Conclusions

Silicon photomultipliers (SiPMs) have undergone a fast development in the last few years and they are currently produced by different manufacturers (Amplification Technologies, id-Quantique, Hamamatsu, Photonique, SensL, Zecotek). Their numerous advantages as compared to other photo detectors, i.e.,high gain, fast timing, compactness, insensitivity to magnetic fields, make them excellent candidates for replacing PMTs and APDs in several applications, in particular for nuclear medicine /11/. In the last year, SiPMs have further improved their characteristics, mainly increasing the photon detection efficiency (PDE) in

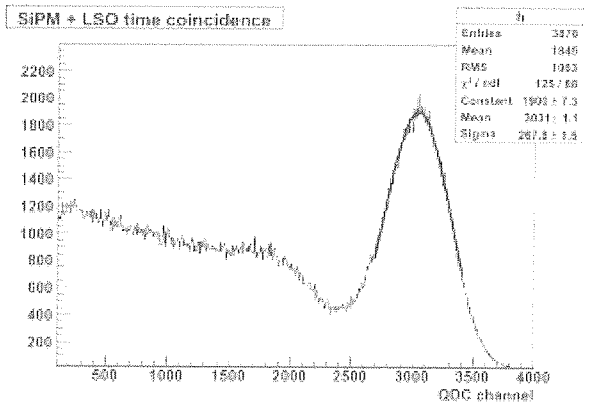

Fig. 28. ^{22}Na (E=511KeV) coincidence spectrumobtained from two SiPM in opposition

the blue region, enlarging the size of the active area and reducing the noise /35/. In the future the technology development will be devoted to the realization of low noise, large area, pixilated detectors /36/. However, it should be emphasized that the exploitation of these detectors will not be possible without a contemporary development of dedicated read-out ASIC chips.

Acknowledgments

I wish to acknowledge Nicoleta Dinu, ClaudioPiemonte (dinu@lal.in2p3.fr - piemonte@fbk.eu) Gabriela Llosa (gabriela.llosa@pi.infn.it) and Marco Petasecca (marcop@uow.edu.au) for helpful discussion and for providing most of the figures reported in this review paper.

References

/1/ K.K.Hamamatsu Photonics, Photomultiplier TubeHandbook, Electron Tube Division, 3rd ed.,2006.

/2/ http://www.electrontubes.com

/3/ http://www.photonis.com,

/4/ K.K. Hamamatsu Photonics, Photodiode TechnicalGuide. http://sales.hamamatsu.com/

/5/ http://www.microphotondevices.com

/6/ K. G. McKay, "Avalanche breakdown in silicon,"Phys. Rev., vol. 94, p.877, 1954.

/7/ M. Singh Tyagi, "Zener and avalanchebreakdown in silicon alloyed p-n junctions" SolidState Electronics, vol. 11, pp. 117-128, 1968.

/8/ F. Zappa et al., "Monolitic active-quencing andactive-reset circuit for single-photon avalanchedetectors", IEEE Journal of Solid-State Circuits,vol.38(7), pp. 1298-1301, 2003

/9/ Z. Sadygov, Russian Patent nr. 2086047 C1,1997.

/10/ V. M. Golovin, et al., Russian Patent nr.1644708, 1999.

/11/ P. Buzhan et al, "Silicon photomultiplier and itspossible applications", Nucl. Instr. Meth A,vol.504, pp. 48-52, 2003

/12/ P. Krizan et al., "Silicon Photomultiplier as adetector of Cherenkov photons", 2007 IEEENucl. Sci. Symposium Conference Record N41-3,pp. 2093-2096, 2007

/13/ http://sipm.itc.it

/14/ N. Dinu et al., "Development of the firstprototypes of silicon photomultiplier (SiPM) atITC-irst", Nucl. Instr. Meth. A, vol.572, pp. 422-426, 2007

/15/ C. Piemonte et al., "Characterization of the firstprototypes of silicon photomultiplier fabricated atITC-irst", IEEE Trans. Nucl. Sci., vol.54, No.1,pp. 236-244, Feb.2007

/16/ A. Lacaita et al., "On the Bremsstralhung originof hot-carrier-induced photons in silicondevices", IEEE Trans. Electron Dev., vol.40, pp.577-582, 1993.

/17/ A. Ingargiola et al., "A new model for opticalcrosstalk in single-photon avalanche diodesarray", 5th Int'l Conference on NewDevelopments in Photodetection, Aix-Les-Bains(France), June 15-20, 2008, electronic fileavailable at http://ndip.in2p3.fr/ndip08/

/18/ B. Dolgoshein, et al., "Large area siliconphotomultipliers: performances and applications",4th Int'l Conference on New Developments inPhotodetection, Beaune (France), June 19-24,2005. Nucl. Instr. and Meth. A 567, pp. 80-82,2005

/19/ W. G. Oldham et al., "Triggering phenomena inavalanche diodes", IEEE Trans. ElectronDevices, vol.ED-19, No.9, pp. 1056-1060, 1972

/20/ . J. McIntyre, "On the avalanche initiationprobability of avalanche diodes above thebreakdown voltage", IEEE Trans. ElectronDevices, vol.ED-20, No.7, pp. 637-641, 1973

/21/ C. Piemonte et al., "New results on thecharacterization of ITC-irst silicon photomultipliers",2006 IEEE Nucl. Sci. Symposium-Conference Record N42-4, pp. 1566-1569, 2006

/22a, 22b/ a) A. Del Guerra, b) R. Battiston, PerugiaWorkshop on Photon Detection, Perugia Italy,June 13-14, 2007 published in: Il NuovoCimento, vol.30-C, No.5, Sept.-Oct.2007.

/23/ M. Petasecca et al., "Thermal and electricalcharacterization of silicon photomultiplier", IEEETrans. Nucl. Sci., vol.55, pp.1686-1690, 2008.

/24/ F. Corsi et al., "Electrical characterization ofsilicon photomultiplier detectors for optimalfront-end design", 2006 IEEE Nucl. Sci.Symposium Conference Record N30-222,pp.1276-1280, 2006

/25/ F. Corsi et al., "Preliminary results from acurrent mode CMOS front-end circuit for siliconphotomultiplier detectors", 2007 IEEE Nucl. Sci.Symposium Conference Record N15-49, pp. 360-365, 2007

/26/ F. Corsi et al., "Modeling a siliconphotomultiplier (SiPM) as a signal source foroptimum front-end design", Nucl. Instr. andMeth. A, vol. 572, pp. 416-418, 2007

/27/ C. Marzocca et al., "Experimental results froman analog front-end channel for siliconphotomultiplier detectors", 2008 IEEE Nucl. Sci.Symposium, Dresden GE, 19-25 Oct. 2008

/28/ C. De la Taille, "SPIROC: Silicon PM ReadoutASIC", 5th Int'l Conference on NewDevelopments in Photodetection, Aix-Les-Bains(France), June 15-20, 2008.http://omega.in2p3.fr

/29/ R. Hawkes et al., "Silicon PhotomultiplierPerformance Tests in Magnetic Resonance PulsedFields", 2007 IEEE Nucl. Sci. Symposium Conf.Record M18-118, pp. 3400-3403, 2007

/30/ D. Renker, "Photo Detectors in High EnergyPhysics", Proceedings of Science: Int'l Workshopon new photon detectors, Kobe (Japan), June 27-29, 2007. http://www-conf.kek.jp/PD07/

/31/ G. Collazuol et al., "Single photon timingresolution and detection efficiency of the IRSTsilicon photo-multipliers" Nucl. Instr. Meth. A,vol.581, pp. 461-464, 2007

/32/ G. Llosa et al., "Silicon photomultipliers andSiPM matrices as photodetectors in nuclearmedicine", 2007 IEEE Nucl. Sci. SymposiumConference Record M14-4, pp. 3220-3223, 2007

/33/ M. Petasecca et al., "Gamma spectroscopyperformance of silicon photomultipliers coupledwith LYSO scintillators", 2008 IEEE Nucl. Sci.Symposium, Dresden GE, 19-25 Oct. 2008

/34/ G. Llosa et al., "Novel silicon photomultipliersfor PET applications", IEEE Trans. Nucl. Sci.,vol.55, pp. 877-881, 2008

/35/ C. Piemonte et al., "Recent developments onsilicon photomultipliers produced at FBK-irst ",2007 IEEE Nucl. Sci. Symposium ConferenceRecord N41-2, pp. 2089-2092, 2007

/36/ N. Dinu et al., "Characterization of a prototypematrix of Silicon PhotoMultipliers (SiPM's)", 5thInt'l Conference on New Developments inPhotodetection, Aix-Les-Bains (France), June 15-20, 2008. http://ndip.in2p3.fr/ndip08/

Giorgio Umberto Pignatel
on behalf of the INFN-DASIPM collaboration
Dept. of Electronic and Information Engineering
DIEI - via G.Duranti 93, 06125 Perugia, Italy
giorgio.pignatel@diei.unipg.it

Prispelo (Arrived): 17.09.2008 *Sprejeto (Accepted): 15.12.2008*